Proceedings World Geothermal Congress 2010
Bali, Indonesia, 25-29 April 2010

Oblique Plate-Slab Subduction Causing Various Anomalous Distributions of Volcanoes and Geothermal Systems in Japan: Simplified Modeling and Simulation

Hiroshi Shigeno

Geological Survey of Japan, AIST, TC-7, 1-1-1 Higashi, Tsukuba, Ibaraki 305-8567, Japan

hiroshi-shigeno@aist.go.jp

Keywords: plate tectonics, oblique subduction, volcano, geothermal system, Kyushu, Kinki, Kanto, Japan, modeling, simulation

ABSTRACT

Various anomalous phenomena are observed at the parts of island arcs and their junctions where oblique plat-slab subduction occurs. In Japan consisting of five island arcs, where the old thick Pacific plate and the young thin Philippine Sea plate have been subducting, various anomalous distributions of volcanoes and geothermal systems are observed at the parts of the oblique subduction as follows: (1) The Kyushu region where the distributions of volcanoes and related geothermal systems have migrated fairly systematically and concentrated in late Neogene to Quaternary time. (2) The Kinki region where high-temperature hot springs distribute on a line in a non-volcanic environment. (3) The Kanto region where a large coastal plain of very low geothermal gradient distributes adjacent to active volcanic belts.

A simple geometry model and simulation method for calculating the slab movement underground have been developed, and applied to the above three regions for better understating the origins of the anomalous phenomena using various kinds of open electronic Earth-sciences information. The corresponding mechanisms have been estimated to be (1) segmentation and steepening of the Philippine Sea plate-slab beneath the north part of the Ryukyu arc, (2) mantle upwelling caused by the deep subduction of the Pacific plate-slab, and segmentation and steepening of the shallow Philippine Sea plate-slab affected by the mantle upwelling under the central part of the Southwest Japan arc, and (3) covering of the segmented Philippine Sea plate-slab from the cold fore-arc region of the Izu-Ogasawara arc over the Pacific plate-slab, respectively.

1. INTRODUCTION

The theory of plate tectonics has been contributing for better understanding of various Earth-scientific phenomena since late 1960's (*e.g.*, Uyeda (1989)). Japanese Islands consisting of five island arcs, namely the Chishima (Kuril), Northeast Japan, Izu-Ogasawara, Southwest Japan and Ryukyu arcs from north, had been settled after the opening of Sea of Japan *ca* 13 Ma. Beneath the five arcs, not only the old thick Pacific (PO, hereafter) plate but also the young thin Philippine Sea (PHS, hereafter) plate have been subducting with the speed of *ca* 10 cm/year and *ca* 4 cm/year probably since *ca* 10 Ma and *ca* 6 Ma, respectively (Fig. 1). Presently, various anomalous distributions of volcanoes, geothermal systems and hypocenters (Figs. 2 and 3) are observed especially at the three regions (nos. 1, 2 and 3 in Figs. 1 to 3) where oblique plate-slab subduction occurs as follows:

(1) The Kyushu region (the north part of the Ryukyu arc): The PHS plate-slab has been subducting obliquely beneath the west part of the Southwest Japan arc adjacent to the Ryukyu arc. Distributions of volcanoes and related geothermal systems at the Kyushu region have migrated fairly systematically from northwest to the southeast direction and concentrated during late Neogene to Quaternary time.

(2) The Kinki region (the central part of the Southwest Japan arc): The PHS and PO plate-slabs have been subducting obliquely beneath the region, and the shallow PHS slab from Nankai Trough is segmented into three around the region. High-temperature hot springs distribute on a line of the NW-SE direction in the Kinki region, although the region, especially the fore-arc part, exists in a non-volcanic environment.

(3) The Kanto region (the southernmost part of the Northeast Japan arc): The PHS and PO plate-slabs have been subducting obliquely beneath the Kanto region, and the shallow PHS slab from Sagami Trough is segmented complicatedly into three. Kanto Plain, the largest coastal plain of Japan, is characterized by the regionally lowest geothermal gradient in Japan, although the area is located adjacent to active volcanic belts.

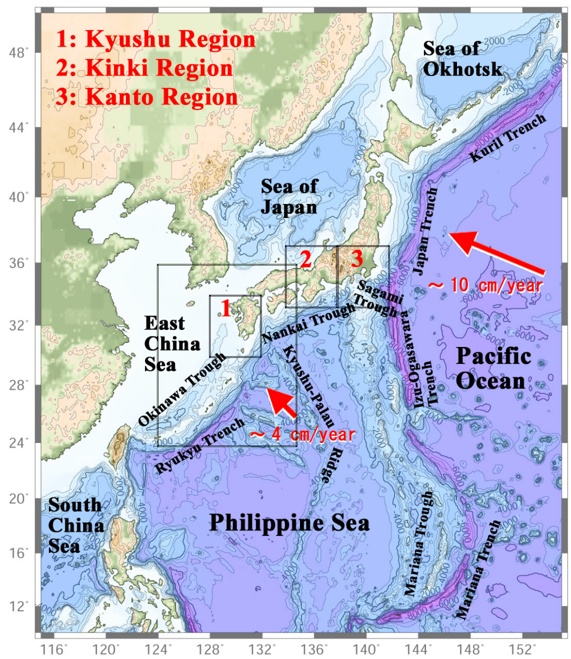

Figure 1: Index map of three studied regions with the relative motion of the Pacific (PO) and Philippine Sea (PHS) plates to Japanese Islands. Geographic map is based on ETOPO5 provided by the U. S. National Geophysical Data Center.

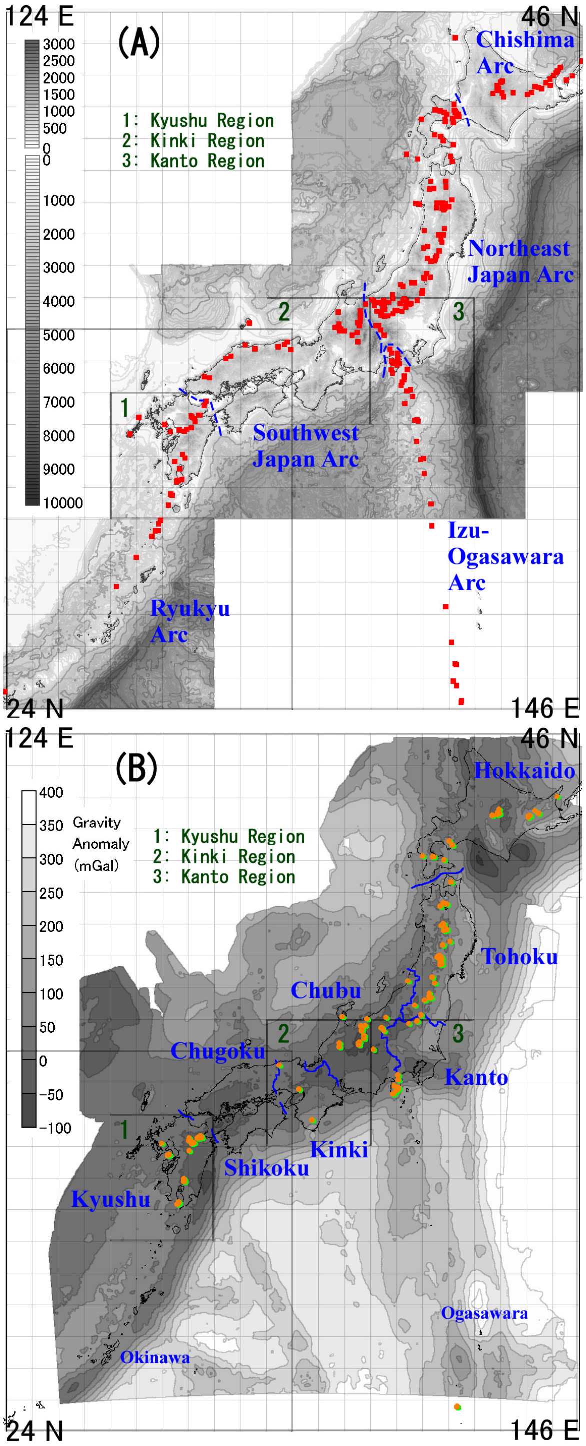

Figure 2: Earth-sciences maps of Japan (modified from Shigeno (2008b)). (A) Geography and Quaternary volcanoes with the boundaries of the five island arcs. (B) Bouguer gravity anomaly and high-temperature hot springs (90 ^{o}C <) with the boundaries of the eight districts of Japan. Refer to Table 1 for the data sources.

In the Geological Survey of Japan (GSJ, hereafter), studies on geothermal resources assessments have been newly conducted using various kinds of electronic geographical and Earth-sciences information which has been openly published since late 1990s by various public organizations. The study results (*e.g.*, GSJ (2007)) including various open-source software developed with Microsoft Visual Basic v.6 could be applied to various kinds of subjects (assessments of resources, environments and hazards) of various areas. Present study has been conducted along the above progress.

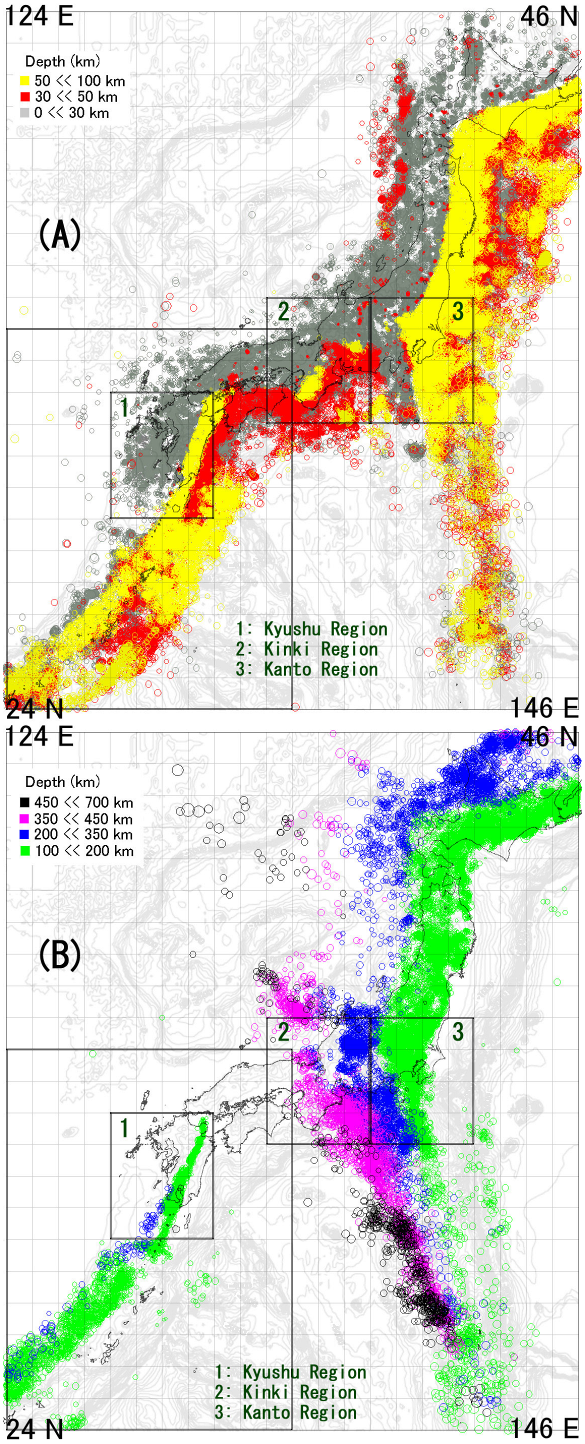

Figure 3: Hypocenter distributions of Japan in 1998-2005 (modified from Shigeno (2008a)). (A) 0 to 100 km depth. (B) 100 to 700 km depth. Deeper hypocenter layers are overlaid, and hide shallower ones partly. Refer to Table 1 and Fig. 1 for the data source and the background map.

In the present article, firstly, a geometric model and simulation method of the obliquely subducting plate-slab will be shown according to Shigeno (2008a). Then, applications of the model and method to the above three regions will be shown on the bases of Shigeno (2008b, 2008c, 2009). Numerous reports concerning the various subjects and areas of this article (*e.g.*, Aoki (1974), and

Utsu (1999); Letouzey and Kimura (1986), Kamata and Kodama (1999), Izawa and Watanabe (2001), and Watanabe (2005); Umeda *et al.* (2004), and Sano and Nakajima (2008); Ishida (1992), Hori (2007), and Niitsuma (2008)) will be seldom referred due to space limitation. Refer to Shigeno (2008a, 2008b, 2008c, 2009) for the details.

Table 1 shows the list of various electronic Earth-sciences information of Japan used in the present study. These numerous data sources are seldom referred in the figures of this article also due to space limitation.

Table 1. List of the electronic Earth-sciences information of Japan used in this study.

Data Item (Abbr.)	References
Quaternary Volcano (QV)	GSJ (2000): Distribution and Occurrence of Cenozoic Volcanic Rocks in Japan, ver. 1.0. DGM G-4.
Thermal Gradient (TG)	GSJ (2004): Geothermal Gradient and Heat Flow Data in and around Japan. DGM P-5.
Hot Spring (HS)	GSJ (2005): Distribution Map and Catalogue of Hot and Mineral Springs in Japan (2nd ed.)(CD-ROM ver.). DGM GT-2.
Heat Flow (HF)	GSJ (2004): Geothermal Gradient and Heat Flow Data in and around Japan. DGM P-5.
Elevation (Elev)	Geographical Survey Institute (1997): Digital Map 250m Grid (Elevation) (CD-ROM).
Bathymetry (SBD)	Japan Oceanographic Data Center (----): 500m Mesh Depth-Sounding Data (J-EGG500) (WWW down load)
Active Fault (AF)	Nakata, T. and Imaizumi, T. (2002): Digital Active Fault Map of Japan (DVD). Tokyo Univ. Press. (ID no.: DAFM0345)
Active Fault (AF)	GSJ (2005): Rupture Probability Map of Major Active Faults in Japan. Tectonic Map, no. 14. (unpublished e-data)
Geology (Geol)	GSJ (1995): Geological Map of Japan 1:,000,000, 3rd ed., CD-ROM ver. DGM G-1.
Gravity (Grav)	GSJ (2000): Gravity CD-ROM of Japan. DGM P-2.
Magnetic Anomaly (AMag)	GSJ (1996): Magnetic Anomaly Map of East Asia 1:4,000,000, CD-ROM ver. DGM P-1.
Hypocenter (EQHC)	Japan Meteorological Agency (2006): The Annual Seismological Bulletin of Japan for 2005 (CD-ROM).

GSJ: Geological Survey of Japan; DGM: Digital Geoscience Map.

2. GEOMETRIC MODEL AND SIMULATION METHOD

Shigeno (2008a) has studied the basic movement of an oceanic plate-slab obliquely subducting beneath an island arc using 3-d Cartesian coordinate system. Fig. 4 shows the very simple geometric model for plate-slab surface using a representative point P (X, Y, Z) moving with a plate (A), and a slab (A1) which has been subducting beneath a fixed island arc from a plate-slab boundary point P_0 (X_0, Y_0, Z_0). Induced simple difference equations for tracing the point position (P_{i-1} -> P_i) changing with time (Δt) are as follows:

$$\Delta X = VA * \Delta t * \cos(\theta A - \theta p) * \cos \theta d$$
$$\Delta Y = VA * \Delta t * \sin(\theta A - \theta p)$$
$$\Delta Z = VA * \Delta t * \cos(\theta A - \theta p) * \sin \theta d$$

$$X_i = X_{i-1} + (-\Delta X * \sin \theta p - \Delta Y * \cos \theta p) * 10^{-5} \text{ (km)}$$
$$Y_i = Y_{i-1} + (\Delta X * \cos \theta p - \Delta Y * \sin \theta p) * 10^{-5} \text{ (km)}$$
$$Z_i = Z_{i-1} - \Delta Z * 10^{-5} \text{ (km)}$$

$$\theta Z_i = -\arctan((X_i - X_0) / (Y_i - Y_0)) - \theta A$$

where VA (cm/year) and θA (°) are speed and direction of movement of the plate A, respectively, and θp (°) and θd (°) are apparent direction angle and dip angle of subduction of the slab A1, respectively. θZ is angle (°) of the horizontal direction of the movement of the slab A1 to the plate A. Refer to Fig. 4 for the direction assignment.

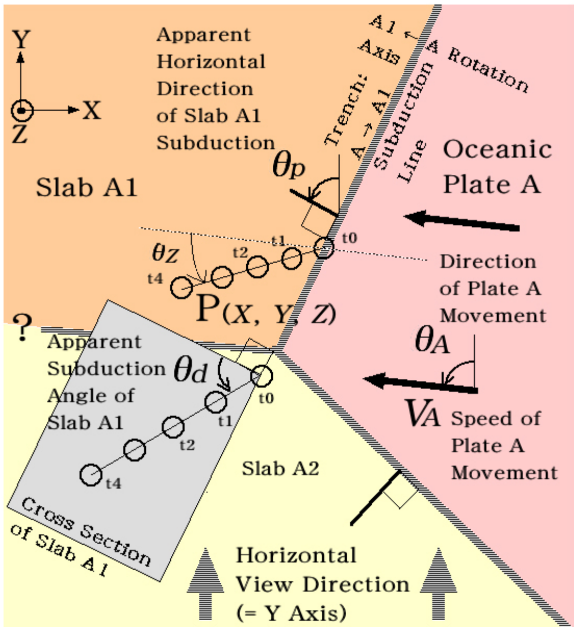

Figure 4: Simplified 3-d model of plate-slab subduction (modified form Shigeno (2008a)). Plane view including a cross-section (gray rectangular).

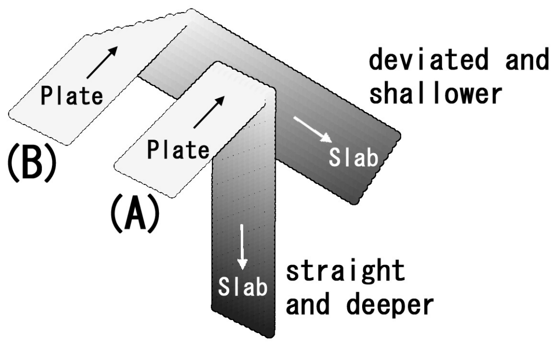

Figure 5: Very simple plate-slab subduction simulated with SSSS (modified form Shigeno (2008a)). (A) Straight (θA - θp = 0°, θd = 90°; θZ = 0°). (B) Oblique (θA - θp = 45°, θd = 90°; θZ = - 45°).

A simple slab subduction simulator, SSSS, has been developed along the above model and equations using Visual Basic v.6. Fig. 5 shows the differences of two vary simple cases of plate-slab subduction simulated with SSSS. Refer to Shigeno (2008a, Figs. 6, 7 and 8) for applications of the simulator to a series of fundamental model cases.

Simulations of the slab surface distributions for the above three regions as well as other areas in Japan have been conducted by roughly matching to the hypocenter distributions (deeper than 30 km; refer to Fig. 3), which probably correspond to the low-temperature slab distributions, through repeatedly adjusting the parameter values of the above equations and Fig. 4.

For the applications of the method, the coordinate system of longitude-latitude is used (*Lon* and *Lat* to *X* and *Y*). The subducting slabs around Japanese Islands generally have a bend between their shallow parts and deep parts at ca 10 to 50 km depth. Two simulation parameters, *Time1* and *Time2* (m.y.), have been used for the times to reach the bending point and the deepest point of the slab, respectively, from the subduction start at trench and trough.

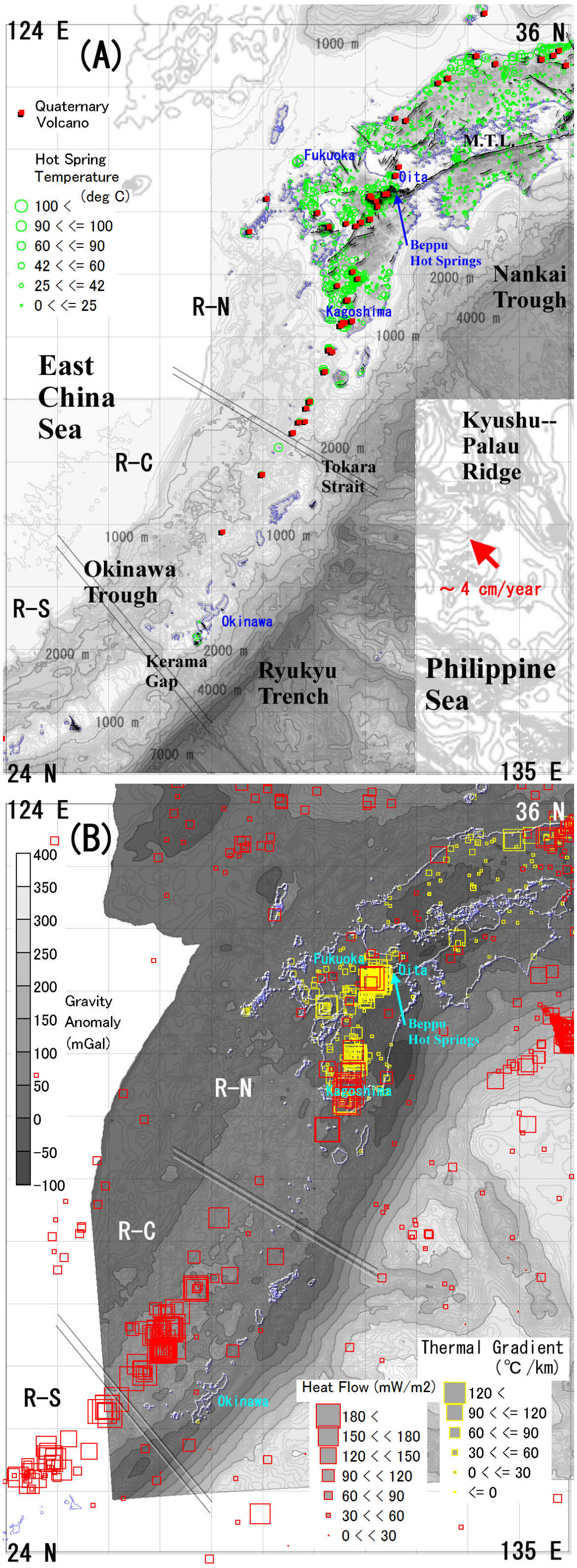

Figure 6: Combined Earth-sciences maps around the Kyushu region, from the south part of the Ryukyu arc to the west part of the Southwest Japan arc (modified from Shigeno (2009)). (A) Geography, active faults, Quaternary volcanoes, and hot springs. (B) Bouguer gravity anomaly, heat flow and geothermal gradient. Refer to Table 1 and Fig. 1 for the data sources.

3. KYUSHU REGION

3.1 Overview of the Kyushu Region

The Ryukyu arc, about 1200 km long, has been classified into three segments, north, central and south (R-N, R-C and R-S, respectively in Fig. 6) based on not only geography but also hypocenter distributions (refer to Figs. 2 and 3). Fig. 3 (B) clearly shows that the deep hypocenter distribution under the north segment (R-N) has a steeper inclination, suggesting that the corresponding slab of the PHS plate is segmented and steepened. The Kyushu region corresponds to the north part of the Ryukyu arc (Fig. 2).

The Ryukyu arc is characterized by the distribution of the long back-arc basin, Okinawa Trough, which is deeper and narrower at the south segment and shallower and wider at the north segment, although the maximum depth of the hypocenters is not so deep (*ca* 300 km depth). Distributions of the high gravity anomalies, submarine volcanoes and hydrothermal systems, and the very high heat flow (Fig. 6) indicate that Okinawa Trough is a newly-developing back-arc basin associated with back-arc magmatism as well as the arc magmatism extended from the Kyushu region (refer to Fig. 6 (A)).

On the other hand, the Southwest Japan arc, especially its west part adjacent to the Kyushu region (the Chugoku-Shikoku zone by Shigeno (2008b)), is mostly non-volcanic (except monogenetic volcanoes at the back-arc region), and lacks in distributions of high-temperature hot-springs and high heat flow (refer to Fig. 6). Also, distribution of active faults is less abundant at the zone, except the long right-lateral transform fault of Median Tectonic Line (M.T.L., hereafter) being active in Quaternary period and continuing to the central part of Kyushu Island (Fig. 6 (A)). The PHS plate-slab has been subducting obliquely to the zone, and the hypocenters distribute shallowly down to *ca* 50 km at the maximum with very gentle inclination under the zone. These are clearly different from those of the Ryukyu arc.

The Kyushu region located at the junction of the Ryukyu arc and the Southwest Japan arc is characterized by intense volcanic and geothermal activities at present time (refer to Fig. 6). There are 17 active volcanoes in the Kyushu region out of 108 in Japan, including five of the most active Class A volcanoes out of 13 according to the definition of the Japan Meteorological Agency.

For hot springs, three prefectures (Oita, Kagoshima and Kumamoto) out of eight in the Kyushu region are ranked in the top five out of 47 prefectures in Japan in terms of total number, total fluid discharge among others according to the statistics of the Japanese Ministry of the Environment. Presently, the Kyushu region shares nearly halves of the number of geothermal power plants, and the total capacity of geothermal power generation in Japan.

The Kyushu region has experienced fairly systematic space-time changes of the volcanic and geothermal activities since *ca* 6 Ma when the present-cycle PHS plate-slab subduction began (refer to Fig. 7 (D) to (A) with time progress). Fig. 7 (A) classifies the Kyushu region into six blocks of different characteristics of the volcanic activities through the time. These are the north (N), east (E), south (S), southwest (R), west (W) and central (C) blocks distributing clock-wisely from north. The width of the E, C and R blocks have been probably enlarged with time as shown by symbol X and white arrows in Fig. 7 (D) to (A).

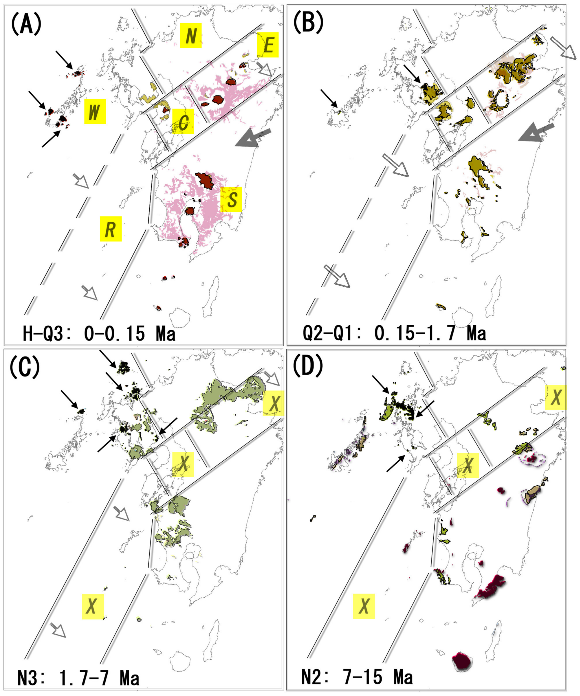

Figure 7: Space-time changes, (D) Middle Miocene to (A) Late Quaternary, of distributions of volcanic rocks in the Kyushu region based on the geologic map by GSJ (1995) (modified from Shigeno (2009)). Refer to text for the letters on yellow patches for six blocks. Small black arrows show alkali rock series. Pinky colors in (B) and (A) show ash-flow deposits. White arrows indicate spreading areas. Gray large arrows mean lateral movement of the fore-arc region. The coast lines are of the present time through (D) to (A).

Table 2. Simulation parameters of slab subduction of the PHS plate beneath the Ryukyu and Southwest Japan arcs (A, *ca* 3 Ma; B, *ca* 0 Ma.).

(A) No	*VA* cm/y	*θA* deg	*Lon0* deg E	*Lat0* deg N	*θp1* deg	*θd1* deg	*Time1* My	*θp2* deg	*θd2* deg	*Time2* My
1	4.0	45	126.5	24.4	42	15	4.0	42	45	7.0
2	4.0	45	127.7	25.4	45	15	4.0	45	45	7.0
3	4.0	45	128.7	26.4	51	15	4.0	51	45	7.0
4	4.0	45	129.7	27.4	51	15	4.0	51	45	7.0
5	4.0	45	130.5	28.4	51	15	4.0	51	45	7.0
6	4.0	45	131.5	29.4	51	15	4.0	51	45	7.0
7	4.0	45	132.0	30.4	54	15	4.0	54	45	7.0
8	4.0	45	132.5	31.4	54	15	4.0	54	45	7.0
9	4.0	45	133.0	32.1	54	15	4.0	54	45	7.0
10	4.0	45	134.1	32.2	30	10	3.0	30	10	3.0
11	4.0	45	135.0	32.4	30	10	3.0	30	10	3.0
12	4.0	45	136.0	32.6	30	10	3.0	30	10	3.0

(B) No	*VA* cm/y	*θA* deg	*Lon0* deg E	*Lat0* deg N	*θp1* deg	*θd1* deg	*Time1* My	*θp2* deg	*θd2* deg	*Time2* My
1	4.0	45	127.0	24.0	40	15	5.0	40	50	10.0
2	4.0	45	128.2	25.0	45	15	5.0	45	50	10.0
3	4.0	45	129.2	26.0	55	15	5.0	55	50	10.0
4	4.0	45	130.2	27.0	55	15	5.0	55	50	10.0
5	4.0	45	131.0	28.0	55	15	5.0	55	65	10.0
6	4.0	45	132.0	29.0	55	15	5.0	55	65	10.0
7	4.0	45	132.5	30.0	60	15	5.0	60	65	10.0
8	4.0	45	133.0	31.0	60	15	5.0	60	65	10.0
9	4.0	45	133.5	31.7	60	15	5.0	60	65	10.0
10	4.0	45	134.1	31.9	30	10	4.0	30	10	6.0
11	4.0	45	135.0	32.3	30	10	4.0	30	10	6.0
12	4.0	45	136.0	32.6	30	10	4.0	30	10	6.0

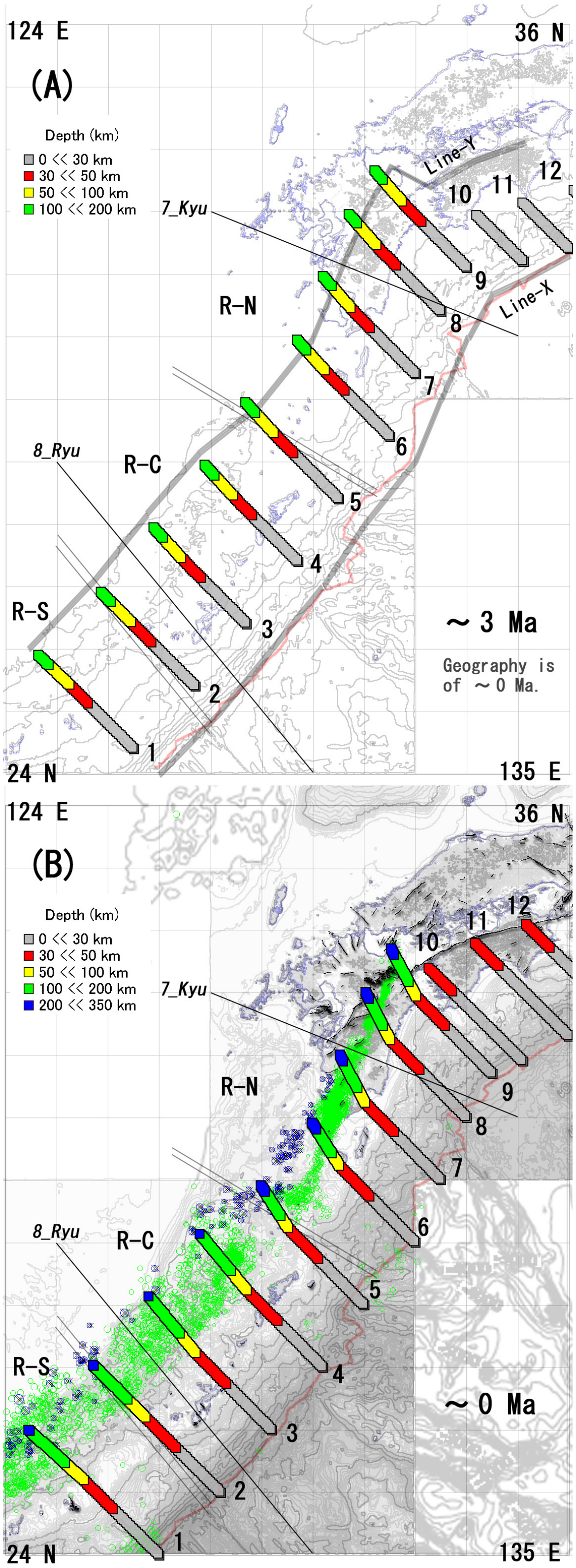

Figure 8: Plane maps of simulated slab subduction of the PHS plate around the Kyushu region (modified form Shigeno (2009)). (A) Results for *ca* 3 Ma. Lines X and Y are the start and end lines, respectively, of the simulated slab for *ca* 0 Ma. (B) Results of *ca* 0 Ma with the hypocenter distributions of 100 to 350 km depth. The geography of (B) is of the present time. Refer to Table 2 for the simulation parameter values, and Figs. 2, 3, 6 and 7 for various Earth-sciences information.

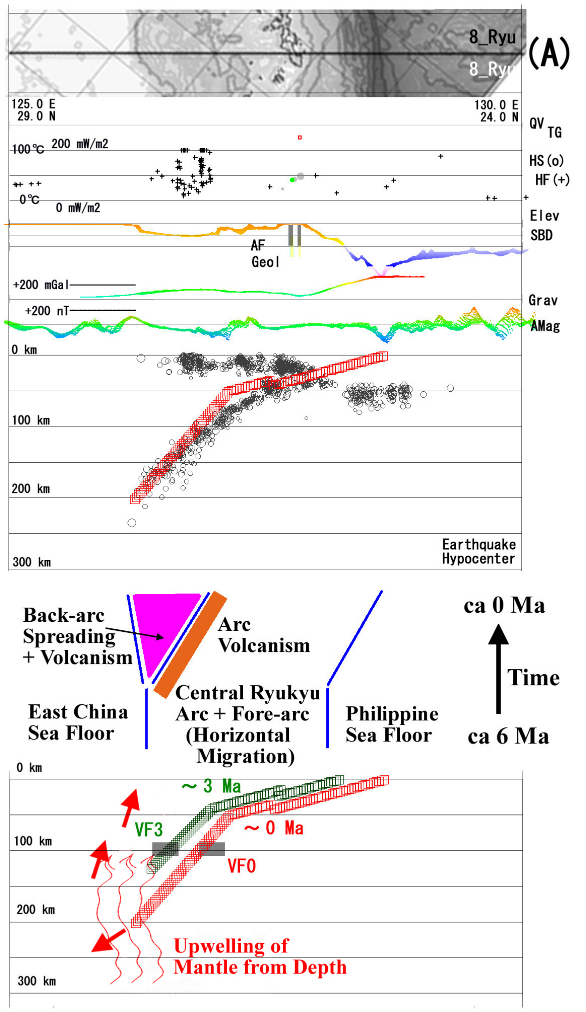

Figure 9: Cross-section (A: 8_Ryu) across Okinawa Island of simulated slab subduction of the PHS plate around the Kyushu region (modified form Shigeno (2009)). Refer to Fig. 8 for the section line. The simulation results for *ca* 3 Ma (green) and *ca* 0 Ma (red) are shown (at the bottom part) with various kinds of Earth-sciences data (at the top pert) and the model of space-time changes (in between). Refer to Table 1 for the data sources.

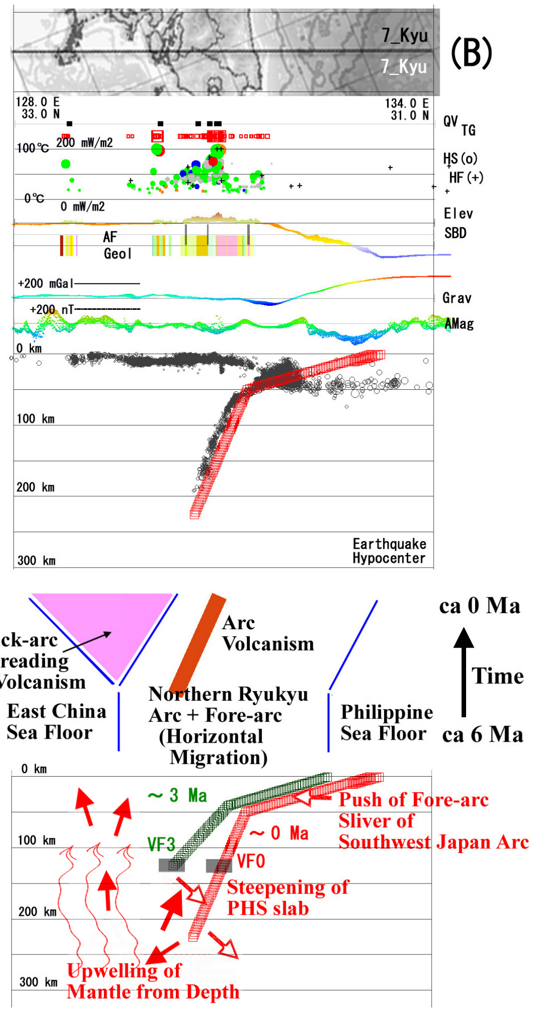

Figure 10: Cross-section (B: 7_Kyu) across the south part of Kyushu Island of simulated slab subduction of the PHS plate around the Kyushu region (modified form Shigeno (2009)). Refer to Fig. 8 for the section line, and refer to the explanation of Fig. 9 for details.

The changes of Fig. 7 (C) to (A) indicate that the arc volcanism in the Kyushu region has migrated to the southeast direction as a whole, and concentrated in Late Quaternary time including the formations of huge amounts of ash-flow deposits and large calderas at the S and E blocks. The above space-time changes of the volcanic activities are expected to be related to the plate-tectonic history of the Ryukyu and Southwest Japan arcs.

3.2 Modeling, Simulation and Discussion of the Plate-Slab Subduction for the Kyushu Region

The above space-time changes of the volcanic activities are modeled and simulated as the consequences of the segmentation and steepening of the PHS plate-slab migrating to the northwest direction with a speed of *ca* 4 cm/year since *ca* 6 Ma. The simulation results of the distributions of the segmented slabs for *ca* 0 Ma and *ca* 3 Ma, using SSSS, by roughly matching to the distributions of the present hypocenters and the past volcanic rocks are shown in Fig. 8 (planes) and Figs. 9 and 10 (cross-sections). The simulation parameter values are given in Table 2.

The very simplified conceptual model for the space-time changes as the basis of the simulation is as follows:

(1) At *ca* 6 Ma, present-cycle migration of the PHS plate-slab began. Probably at the time, the slab beneath the Southwest Japan arc was *ca* 0 km long, but the slab beneath the Ryukyu arc was *ca* 160 km long due to the different histories of the past-cycle subduction beneath the two arcs (this effect was included in the simulation by changing the parameter values of *Time1* and *Time2* in Table 2). The back-arc volcanism at the W block in the Kyushu region had continued by the effect of the previous PHS plate-slab subduction terminated *ca* 12 Ma, though the arc volcanism had a long interruption in other blocks (Fig. 7 (D) to (C)).

(2) At *ca* 4 Ma to 3 Ma, the subducting front edge of the slab beneath the Ryukyu arc reached *ca* 100 km depth, and began to cause intense arc magmatism probably through the Ryukyu arc, especially in the E, W and S blocks in the Kyushu region (refer to Fig.7 (C)). However, at the central to south segments of the Ryukyu arc, back-arc magmatism (mantle upwelling) occurred probably with the arc magmatism due to the special conditions of the area (possibly related to the previous subduction history, crust conditions of the thick sedimentary shelf continued from East China Sea, and/or others). This caused thinning of the

crust, namely opening of Okinawa Trough, through the back-arc region of the Ryukyu arc, and segmentation of the Ryukyu arc (R-N, R-C and R-S as shown in Figs. 6 and 8) including the Kyushu region (Fig. 7 (C)) (Shigeno, 2008a, 2009). The Ryukyu arc, including the subduction line at Ryukyu Trench, began to migrate to the southeast direction with a speed of *ca* 2 cm/year (this effect to simulation was adjusted by changing the parameter values of the start position of subduction, *Lon0* and *Lat0*, in Table 2 (A)).

(3) At *ca* 2 Ma, the obliquely subducting front edge of the slab of the PHS plate beneath the Southwest Japan arc reached under Shikoku Island, and the right-lateral movement of the for-arc region along M.T.L. began. This caused a collision of the crusts of the south part of Shikoku Island and the central-south part of Kyushu Island (shown by a large gray arrow in Fig. 7 (B)) associated with migration speed decrease of the part in the Kyushu region, and the slab beneath the Kyushu region began to steepen (by coupling of the crust and the shallow part of the slab). As a result, the arc volcanism has migrated to the southeast direction at the S and E blocks, and from the W to C blocks, forming a large graben through the E to C blocks (continuing to the R block and Okinawa Trough), in the Kyushu region (Fig. 7 (B)). The spreading of Okinawa Trough, the migration to the southeast direction of the Ryukyu arc, and its segmentation have continued with the back-arc and arc volcanism, but the slab steepening has not been caused at the R-C and R-S regions located far away from the Southwest Japan arc.

(4) Since *ca* 0.2 Ma, the continued slab steepening caused very intense volcanism at the S and E blocks in the Kyushu region, including voluminous ash-flow eruption and large caldera formation at the narrow areas (Figs. 7 (A), 8 (B) and 10). The back-arc volcanism being continued at the W block (Fig. 7 (A)) has probably been pushed westward due to the mantle upwelling affected by the crust collision and slab steepening. The R-C and R-S regions of the Ryukyu arc, however, have continued the above activities of (3).

The above model and the simulation results (Figs. 8, 9 and 10) are fairly concordant to the observed phenomena (Figs. 2, 3, 6 and 7). The present intensive geothermal activities in the Kyushu region associated with the Quaternary volcanic activities, especially the most prominent discharge of Beppu Hot Springs in Japan (See Fig. 2 (A)), could be explained fairly well by the above results of this study. However, there remain many questions to be solved with information would be obtained in future. These are, for example, other possibilities of the mechanisms for the slab steepening beneath the Kyushu region, the formation mechanism of Okinawa Trough, the formation mechanism of the graben at the E to C blocks in the region, the consistency of the movement of the PHS plate since *ca* 6 Ma among others.

4. KINKI REGION

4.1 Overview of the Kinki Region

Shigeno (2008a, 2008b) divided the Southwest Japan arc into three zones, namely Chubu, Kinki and Chugoku-Shikoku, with two tectonic lines of the NW-SE direction, namely the Tsurugawan-Isewan line and the Oki East-Shionomisaki Canyon line, based on the distributions of geography, gravity anomaly, active faults and hypocenters. Refer to Fig. 11 for various Earth-sciences information for the Kinki zone (region). The Kinki region is characterized by the distributions of a regional depression zone (probably a graben) of the NW-SE trend including Wakasawan (bay), Biwako (lake) and Isewan (bay), and the Ria-type coast lines at the east part, and high-temperature (90 °C <) hot springs, namely Yumura, Arima and Yunomine Hot Springs distributed on a NW-SE line at the west part.

In Japanese Islands, almost all of the high-temperature hot springs are associated with the Quaternary volcanoes, whose magma chambers and their consolidated igneous bodies underground could be efficient sources of heat and high-temperature fluids. However, the Kinki region is unique on the point that the high-temperature hot springs are distributed, especially at its south part (fore-arc area), without the association of the Quaternary volcanoes as shown in Fig. 2 (A) and (B).

Another special point of the Kinki zone is that the deepest hypocenter corresponding to the PHS plate-slab there is *ca* 75 km depth, which is clearly deeper than *ca* 50 km depth observed at the Chubu and Chugoku-Shikoku zones (refer to Fig. 3 (A)). This means that the slab of the PHS plate beneath the Southwest Japan arc is segmented into three, and the slab dip-angle under the Kinki zone is steeper than those of the two other zones. The zigzag distributions of the hypocenters beneath the Southwest Japan arc (Fig. 3 (A)) reflect the segmentation.

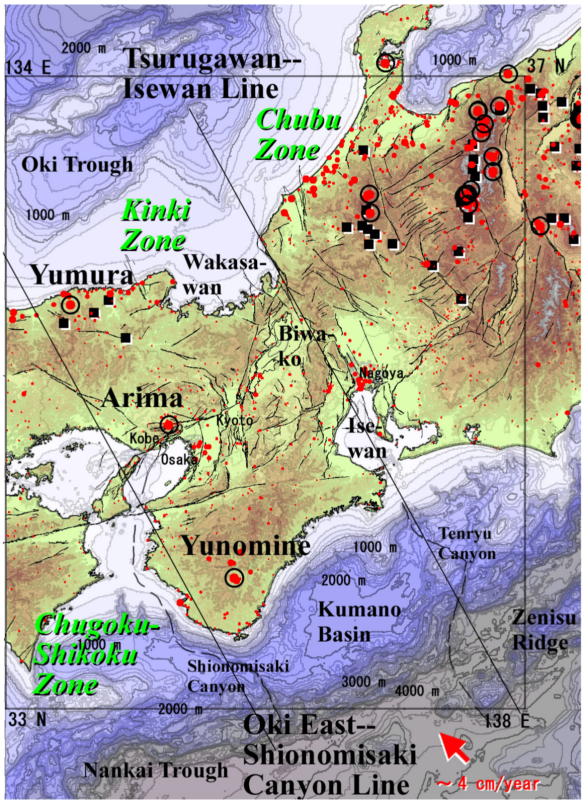

Figure 11: Integrated Earth-sciences map around the Kinki region including Quaternary volcanoes (black square), hot springs (red circle) and active faults (modified from Shigeno (2008b)). High-temperature hot springs (90 °C <) are marked by large open circles. Two tectonic lines dividing the three zones of the Southwest Japan arc are shown by dotted lines along the sea-bottom geography for the south parts. Refer to Table 1 for the data sources.

Table 3. Simulation parameters of plate-slab subduction beneath the Kinki region (A, PO plate-slab; B, PHS plate-slab).

(A) No	VA cm/y	θA deg	Lon0 deg E	Lat0 deg N	θp1 deg	θd1 deg	Time1 My	θp2 deg	θd2 deg	Time2 My
1	10.0	70	143.0	29.0	110	10	1.5	110	65	8.0
2	10.0	70	142.5	30.0	110	10	1.5	110	62	8.0
3	10.0	70	142.0	31.0	100	10	1.0	100	55	8.0
4	10.0	70	142.0	32.0	90	10	1.0	90	41	8.0
5	10.0	70	142.0	33.0	90	10	1.0	90	40	8.0
6	10.0	70	142.0	33.8	110	10	2.0	110	60	9.0
7	10.0	70	142.0	34.0	90	15	2.0	90	35	8.0
8	10.0	70	142.0	35.0	80	15	2.0	80	35	8.0
9	10.0	70	142.5	36.0	60	15	2.0	60	35	8.0

(B) No	VA cm/y	θA deg	Lon0 deg E	Lat0 deg N	θp1 deg	θd1 deg	Time1 My	θp2 deg	θd2 deg	Time2 My
10	4.0	45	134.1	31.9	30	10	4.0	30	10	6.0
11	4.0	45	135.0	32.3	30	10	4.0	30	10	6.0
12	4.0	45	136.0	32.6	30	10	4.0	30	10	6.0
13	4.0	45	137.0	33.0	30	10	4.0	30	45	6.0
14	4.0	45	137.5	33.3	30	10	4.0	30	45	6.0
15	4.0	45	138.0	33.7	45	10	4.0	45	10	6.0
16	3.0	45	138.5	34.5	80	25	4.0	80	25	6.0
17	3.0	45	139.3	35.0	−80	25	4.0	−80	25	6.0

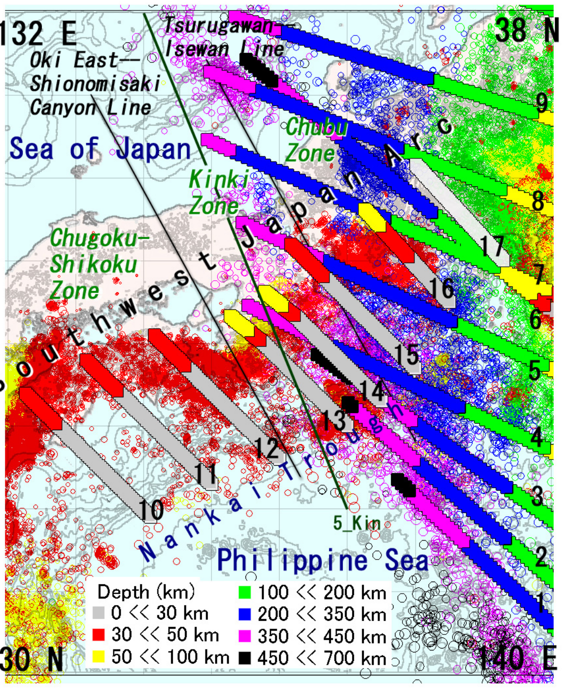

Figure 12: Combined plane map of deep hypocenter distribution and simulated slab subduction of the PO and PHS plates around the Kinki region (modified form Shigeno (2008b)). Refer to Table 3 for the simulation parameter values.

4.2 Modeling, Simulation and Discussion of the Plate-Slab Subduction for the Kinki Region

The simulation results of the distributions of the slabs of the PO and PHS plates, using SSSS, by roughly matching to the distributions of the hypocenters are shown in Fig. 12 (plane) and Fig. 13 (A) (cross-section with explanation). The simulation parameter values for the two plate-slabs are given in Table 3.

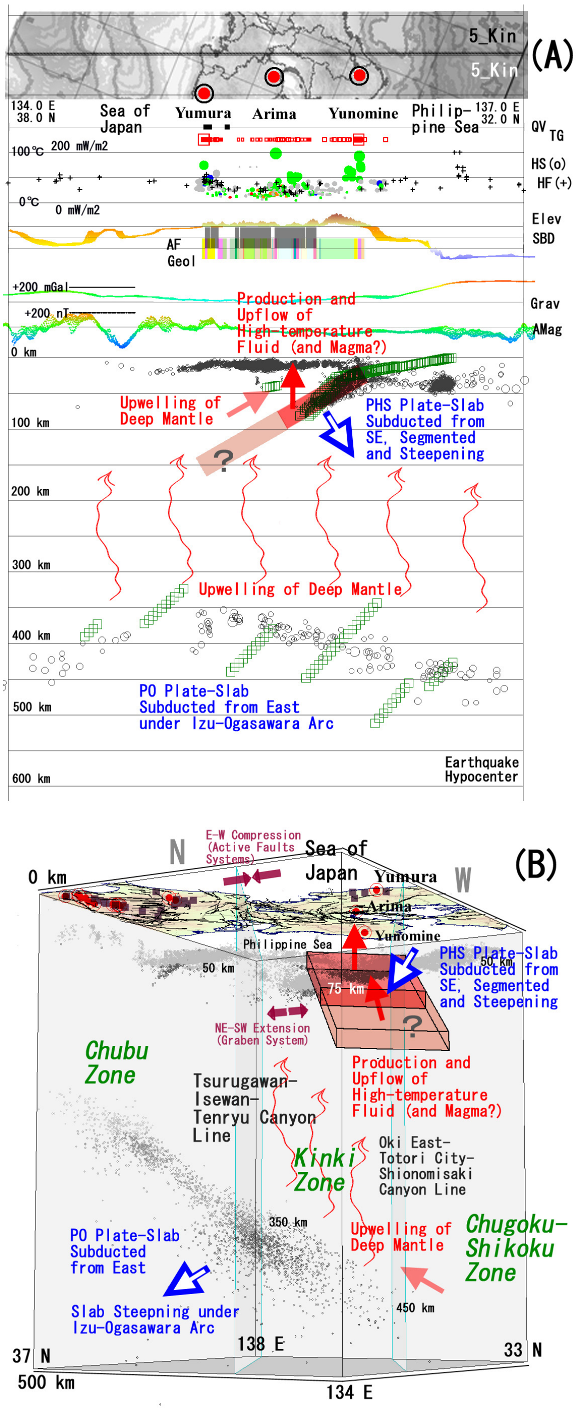

Figure 13: Simulated plate-slab subduction for the Kinki region, and explanation of model for the formation of the high-temperature hot springs (modified form Shigeno (2008b)). (A) Cross-section along 5_Kin (refer to Fig. 12), including various Earth-sciences information. (B) 3-d "mole" view from the northwest direction and *ca* 400 km depth (refer to Fig. 11 for the mapped area). Refer to Table 1 for the data sources.

Fig. 13 also shows the model induced from the overviewed phenomena for the formation and distribution of the high-temperature hot springs at the Kinki region. The fairly simplified conceptual model as the basis (and the result) of the simulation study is as follows:

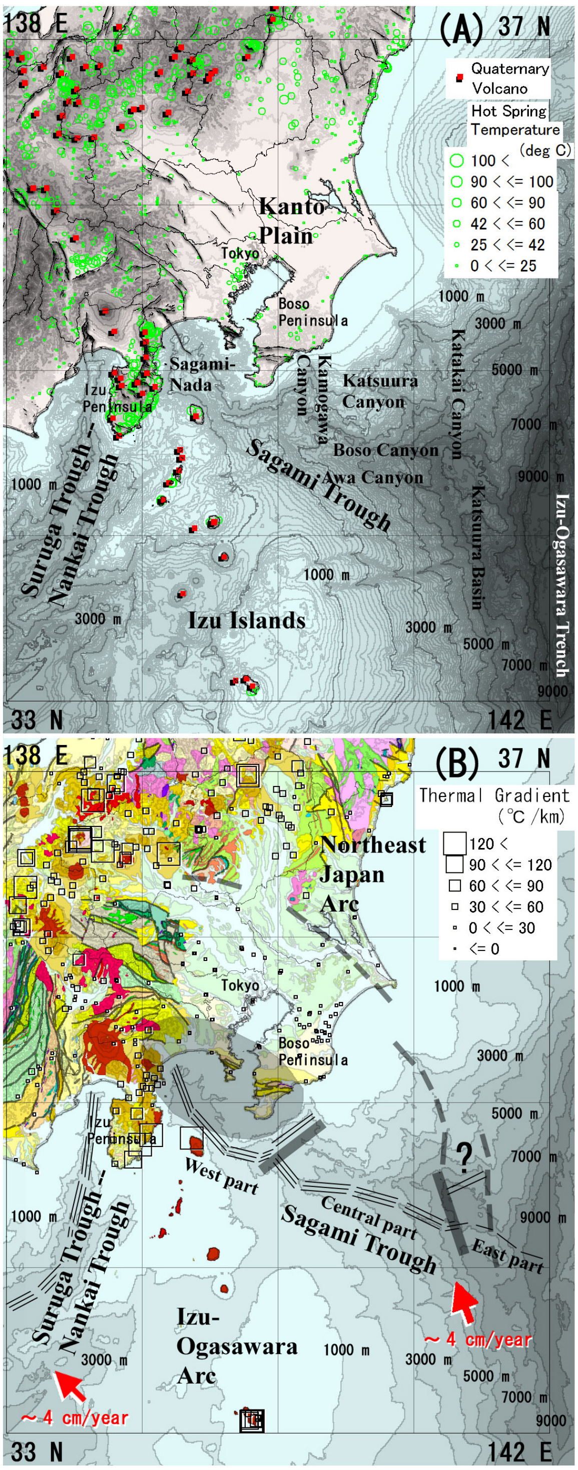

Figure 14: Combined Earth-sciences maps for the Kanto region (modified from Shigeno (2008c)). (A) Geography, active faults, Quaternary volcanoes, and hot springs. (B) Geology and geothermal gradient, and the division model of Sagami Trough. Gray ellipse corresponds to the crustal movement area by the great Kanto earthquakes in 1703 (*ca* M 8.1) and 1923 (*ca* M 7.9). Refer to GSJ (1995) for the legend of geology (Kanto Plain is covered mostly by Quaternary sedimentary rocks). Refer to Table 1 for the data sources.

(1) The deepest part (*ca* 450 km depth) of the thick slab of the PO plate subducted under the Izu-Ogasawara arc is distributed beneath the Kinki region. This slab has caused the upwelling of hot upper mantle from the depth (related to the depression and possibly to a beginning of back-arc volcanism) beneath the Kinki zone.

(2) The hot (and less dense) mantle upwelling has caused the segmentation (into three along the two tectonic lines) and steepening (*ca* 45^{o}), with a slight deviation to the west, of the slab of the PHS plate beneath the Kinki region. As a result of this dip-angle steepening, another up-flow of the hot upper mantle has occurred obliquely from the northwest to the gradually opening mantle wedge just under the west part of the Kinki region.

(3) The two-side heating (from the bottom and the top surfaces) of the segmented PHS slab beneath the west part of the Kinki region has probably caused not only subducted fluid migration from the slab to the crust partly trough the mantle wedge, but also magma generation, although the slab depth is fairy shallow.

The crust conditions are regionally and locally complex and not so clearly understood, including the distributions of various kinds of faults at the Kinki region. Hence, it is difficult to discuss about the local distributions of the high-temperature hot springs. However, the above model and simulation result seem to explain fairly well the regional formation mechanism of the anomalous distributions of the high-temperature hot springs at the Yunomine, Arima and Yumura areas in the west part of the Kinki region.

5. KANTO REGION

5.1 Overview of the Kanto Region

The Kanto region, which is located at the southernmost part of the Northeast Japan arc, is complicated due to the distributions of the two subduction systems: the PO plate-slab from Izu-Ogasawara Trench on the east to southeast side, and the PHS plate-slab from Sagami Trough on the south to southeast side (Fig. 14). Kanto Plain, which is centered by the Tokyo metropolitan area, is the largest plain in Japan, and has *ca* 4 km-thick (at maximum) Neogene-Quaternary sedimentary rocks in a basin structure.

The Izu-Ogasawara arc, which is located near the east rim of the PHS plate with semi-continental characteristics, has migrated from the south, and collided to the junction of the Southwest and Northeast Japan arcs around Izu Peninsula. As a result, a long trench of the WSW-ENE direction previously existed at the north of the Izu-Ogasawara arc has been bended and divided into Suruga-Nankai Troughs and Sagami Trough presently extending to the different directions (*e.g.*, Niitsuma (2008); refer to Fig. 14).

The hypocenter distribution at the Kanto region is complex due to the above complex plate boundaries of the subduction and collision (at the north of Izu Peninsula) associated with transform (right-lateral slip along the west part of Sagami Trough). Fig. 15 shows complex four-layered oblique distribution of hypocenters along a NW-SE cross-section. The bottom two layers correspond to the slab of the PO plate (*ca* 80 km thick), and the top two layers (the topmost one is actually a dotted layer of clusters) correspond to the slab of the PHS plate (*ca* 30 km thick). This double layering of the PHS plate-slab has not been observed beneath the Southwest Japan and Ryukyu arcs.

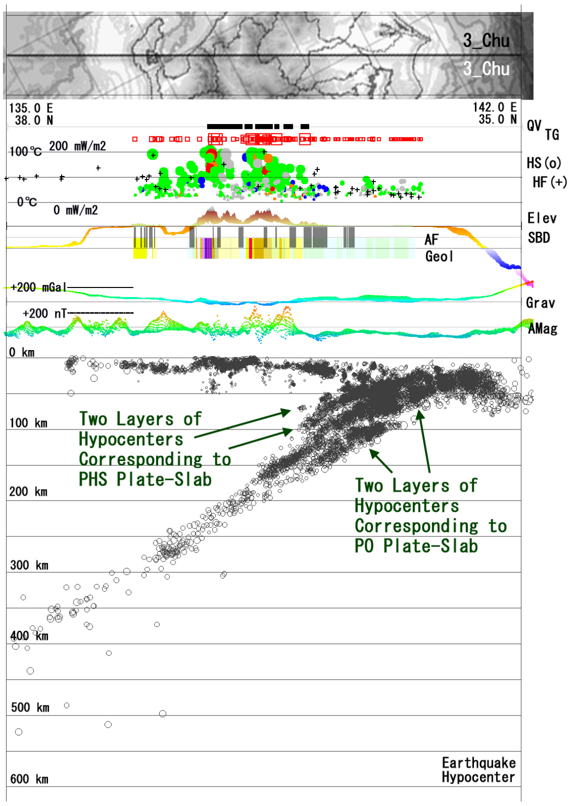

Figure 15: NW-SE Cross-section through the Kanto region, from Sea of Japan to Pacific Ocean (modified from Shigeno (2008c)). Refer to Table 1 for various Earth-sciences information.

Table 4. Simulation parameters of segmented slab subduction of the PHS plate from Sagami Trough beneath the Kanto region (W, from the west part; C, from the central part; E, from the east part).

(W) No	VA cm/y	θA deg	Lon0 deg E	Lat0 deg N	θp1 deg	θd1 deg	Time1 My	θp2 deg	θd2 deg	Time2 My
1	2.0	20	139.4	34.9	−70	10	2.0	−70	40	6.0
2	3.0	20	139.6	34.7	20	10	3.0	20	34	6.0
3	3.0	20	139.7	34.7	20	10	3.0	20	33	6.0
4	3.5	20	139.8	34.8	20	10	2.8	20	32	5.0
5	3.5	20	139.9	34.8	20	10	2.8	20	31	5.0
6	4.0	20	140.0	34.8	20	10	2.5	20	30	4.0
7	4.0	20	140.1	34.8	20	10	2.5	20	29	4.0
8	4.0	20	140.2	34.9	20	10	2.5	20	28	4.0
9	4.0	20	140.3	34.9	20	10	2.5	20	27	4.0

(C) No	VA cm/y	θA deg	Lon0 deg E	Lat0 deg N	θp1 deg	θd1 deg	Time1 My	θp2 deg	θd2 deg	Time2 My
1	4.0	20	140.1	34.6	−20	12	2.5	−20	45	6.0
2	4.0	20	140.2	34.6	−20	12	2.7	−20	43	6.0
3	4.0	20	140.3	34.5	−20	12	2.8	−20	41	6.0
4	4.0	20	140.4	34.5	−20	12	3.0	−20	39	6.0
5	4.0	20	140.5	34.5	−20	12	3.2	−20	37	6.0
6	4.0	20	140.6	34.4	−20	12	3.3	−20	35	6.0
7	4.0	20	140.7	34.4	−20	10	3.5	−20	33	6.0
8	4.0	20	140.8	34.4	−20	10	3.7	−20	30	6.0
9	4.0	20	140.9	34.3	−20	10	3.8	−20	27	6.0
10	4.0	20	141.0	34.3	−20	10	4.0	−20	24	6.0
11	4.0	20	141.1	34.3	−20	10	4.2	−20	21	6.0
12	4.0	20	141.2	34.2	−20	10	4.3	−20	18	6.0
13	4.0	20	141.3	34.2	−20	10	4.5	−20	15	6.0

(E) No	VA cm/y	θA deg	Lon0 deg E	Lat0 deg N	θp1 deg	θd1 deg	Time1 My	θp2 deg	θd2 deg	Time2 My
1	4.0	20	141.3	34.4	20	8	4.5	20	10	6.0
2	4.0	20	141.4	34.5	20	8	4.5	20	10	6.0
3	4.0	20	141.5	34.5	20	8	4.5	20	10	6.0

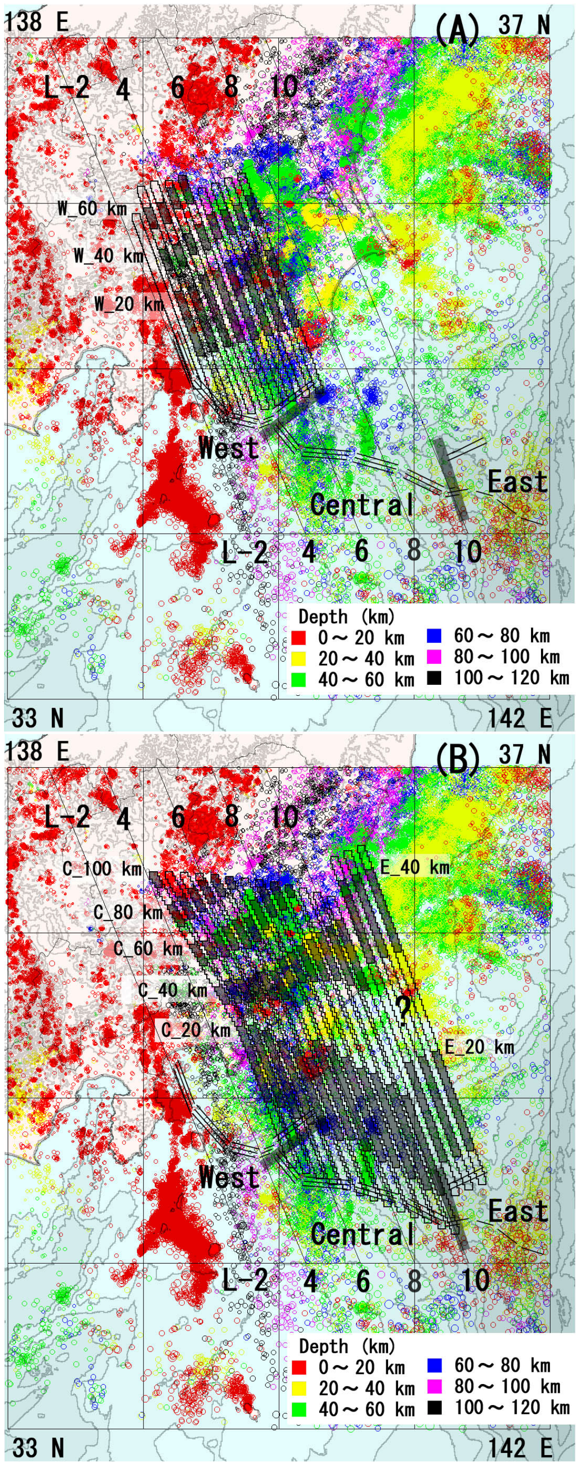

Figure 16: Integrated plane maps of hypocenter distribution and simulated segmented-slab subduction of the PHS plate for the Kanto region (modified form Shigeno (2008c)). (A) Simulation results for the segmented slab from the west part of Sagami Trough. (B) Simulation results for the segmented slabs from the central and east parts of Sagami Trough. Refer to Table 4 for the simulation parameter values, and refer to Fig. 14 for various Earth-sciences information.

Figs. 14 and 15 show that Kanto Plain is characterized by the regionally lowest geothermal gradient (*ca* 20 °C/km) in Japan, and no distribution of high-temperature (42 °C <) "hot springs" (most of them are artificially produced by well drilling). The Quaternary volcanoes are distributed to the west and northwest, although the depth of the top surface of PO slab is deeper than 100 km at the west to northwest part of Kanto Plain.

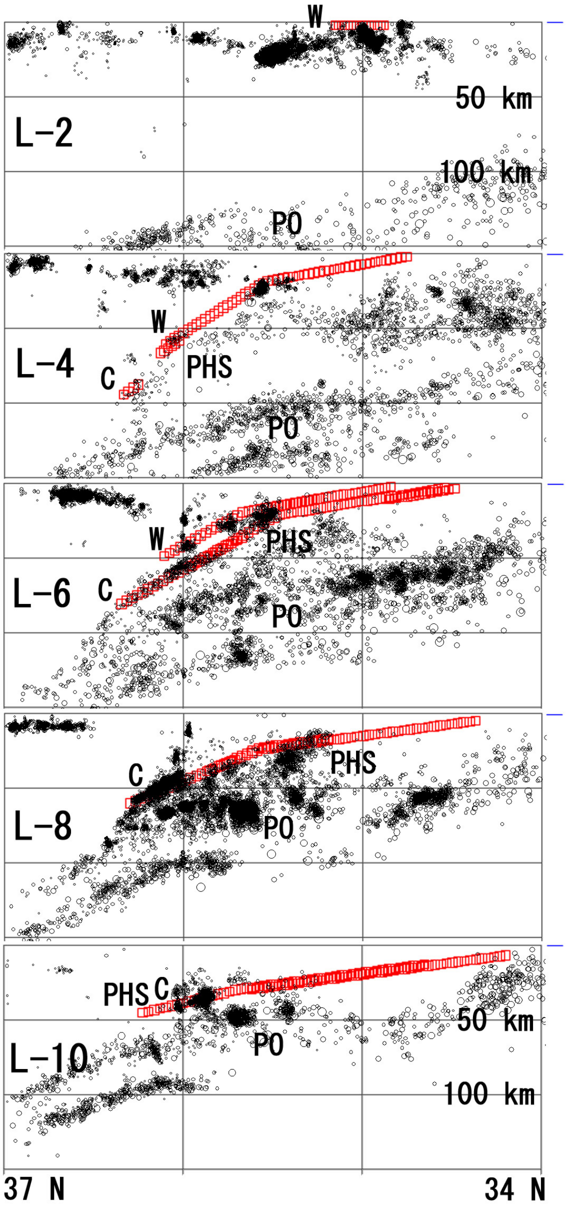

Figure 17: Cross-sections of simulated segmented-slab subduction of the PHS plate for the Kanto region with hypocenter distribution (modified form Shigeno (2008c)). Refer to Fig. 16 for the section lines, L-2 to L-10, and refer to Table 4 for the simulation parameter values. PO, PHS, W and C indicate the plate-slabs and slab segments corresponding to the hypocenter distributions.

5.2 Modeling, Simulation and Discussion of the Plate-Slab Subduction for the Kanto Region

The simulation results, using SSSS, of the PHS plate-slab subduction from Sagami Trough since *ca* 6 Ma by roughly matching to the hypocenter distributions are shown in Fig. 16 (two planes) and Fig. 17 (five cross-sections). The simulation parameter values are given in Table 4. The bathymetry of the subduction start points along Sagami Trough has also been used as a parameter of the simulation, because its effect is relatively large in this case (but omitted from Table 4).

The fairly simplified conceptual model as the basis of the simulation, and the induced slab distributions as the results are as follows:

(1) The PHS plate along Sagami Trough has been migrating from the SSE direction (parallel to Izu-Ogasawara Trench) with a speed of *ca* 4 cm/year without the effect of spreading (E-W direction) of the back-arc area of the Izu-Ogasawara arc. At and around the collision and transform boundaries, however, the speed is probably much slower.

(2) The slab of the PHS plate subducting from Sagami Trough has been segmented into three (the west, central and east parts; Fig. 14 (B)) reflecting the above geographical and historical complexity.

(3) The west segment, as a branch of the central segment, has been subducting around the south part of Boso Peninsula associated with a transform plate boundary along the west part of Sagami Trough. This segmented thin slab lies beneath the southwest half of Kanto Plain down to *ca* 70 km depth (refer to Fig. 17, L-2 to L-6) corresponding to the surface distributions of the active faults (Fig. 14 (A)).

(4) The central segment has been subducting from the central part of Sagami Trough under the west segment and beneath most part of Kanto Plain. Its deepest part reaches *ca* 100 km depth under the northwesternmost corner of the plain (refer to Fig. 17, L-4 to L-10). This segment with a relatively high dip angle, is slightly deviated westward due to the oblique slab subduction (refer to Figs. 16 (B) and 17).

(5) The east segment is estimated to have been subducting from the east part of Sagami Trough, where sea-bottom topography is very complex near Izu-Ogasawara Trench. Here, the slab, which is distributed above the shallow surface of the slab of the PO plate, is probably very thin and narrow, and has a gentle inclination (refer to Figs. 16 (B)).

The above model and the simulation results indicate that the three segmented slabs of the PHS plate, which correspond uniquely to the cold fore-arc region of the Izu-Ogasawara arc, have widely lain over the surface of the slab of the PO plate subducting beneath. This probably causes the distribution of anomalously low geothermal gradient, and the absence of the high-temperature “hot springs” in Kanto Plain. Also, this probably causes the distributions of Quaternary volcanoes at the adjacent areas to the west and northwest where the segmented slabs of the PHS plate are probably not extended, and the slab of the PO plate is directly distributed at the depth deeper than 100 km.

CONCLUSIONS

Various anomalous phenomena are observed at the parts of island arcs and their junctions where oblique plat-slab subduction occurs. In this article, very simple geometric modeling and simulation method for the oblique subduction have been applied to the three regions with anomalous distributions of volcanoes and geothermal systems in Japan using various kinds of open electronic Earth-sciences information.

(1) For the Kyushu region, the segmentation and steepening of the PHS plate-slab beneath the north part of the Ryukyu arc explain the distributions of volcanic and geothermal activities which have migrated fairly systematically and concentrated during the late Neogene to Quaternary time. The transform movement of the for-arc region of the Southwest Japan arc produced by the oblique subduction of

the PHS plate-slab probably has caused the steepening (Figs. 6, 7, 8, 9 and 10).

(2) For the Kinki region, mantle upwelling caused by the deep subduction of the PO plate-slab, and the segmentation and steepening of the shallow PHS plate-slab affected by the above mantle upwelling beneath the central part of the Southwest Japan arc explain the aligned distribution of the high-temperature hot springs in a non-volcanic environment (Figs. 11, 12 and 13).

(3) For the Kanto region, the three segmented slabs of the PHS plate produced from the cold fore-arc region of the Izu-Ogasawara arc covering over the PO plate-slab probably explain the regionally lowest geothermal gradient of Kanto Plain in Japan (Figs. 14, 15, 16 and 17).

The modeling and simulation method as well as the case study results of this article could be applicable to various plate-slab subduction (also possibly to various plate collision and transform) boundary areas of the world. It is a limitation that the method estimates directly only the geometry and movement of the plate-slab, not those of the crust where volcanoes and geothermal systems develop. But, the application could be very much helpful for better understanding the nature of volcanic and geothermal systems anomalously distributed there.

ACKNOWLEDGEMENT

I would like to thank Dr. Mitsuru Nakagawa (GSJ; Hokkaido Center, AIST) for commenting on the manuscripts in Japanese, and Dr. Sachihiro Taguchi (Fukuoka University) for giving an inspiration to the case study for the Kyushu region. I would like to extend my thanks to the people sincerely providing various kinds of open electronic Earth-sciences information of Japan.

REFERENCES

Aoki, H.: Plate tectonics of arc-junction at Central Japan. *Jour. Phys. Earth*, **22**, (1974), 141-161.

Geological Survey of Japan: *Geothermal Data Processing Collections for the Hohi, Oita, and Kyushu areas, Japan: Report, and Data and Program collections of Simplified Integrated-Processing for the "Study on Geothermal Resources Assessments using GIS (FY2001-2005)" (CD-ROM)*. DGM GT-3, (2007). (in Japanese with English abstract)

Hori, S.: Seismic activity associated with the subducting motion of the Philippine Sea plate beneath the Kanto district, Japan. *Tectonophysics*, **417**, (2007), 85-100.

Ishida M.: Geometry and relative motion of the Philippine Sea plate and Pacific plate beneath the Kanto-Tokai district, Japan. *Jour. Geophy. Res.*, **97**, (1992), B489-513.

Izawa, E. and Watanabe, K.: Overview of epithermal gold mineralization in Kyushu, Japan. *Society of Economic Geologists Guidebook Series*, **34**, (2001), 11-15.

Kamata, H. and Kodama, K.: Volcanic history and tectonics of the Southwest Japan Arc. *The Island Arc*, **8**, (1999), 393-403.

Letouzey, J. and Kimura, M.: The Okinawa trough: Genesis of a back-arc basin developing along a continental margin. *Techtonophysics*, **125**, (1986), 209-230.

Niitsuma, N.: *Plate Tectonics –The New Advance and Japanese Islands–*. Kyoritsu Shuppan. 292p, (2008). (in Japanese with English title)

Sano, Y. and Nakajima, J.: Geographical distribution of $^3He/^4He$ ratio and seismic tomography in Japan. *Geochem. Jour.*, **42**, (2008), 51-60.

Shigeno, H.: Study on high-temperature hot-springs in the Kinki district, Japan, based on integrated analysis of electronic earth-sciences information (1): Simplified mathematical model and numerical simulation of oblique oceanic plate-slab subduction. *Chishitsu News*, no. 646, (2008a), 6-21. (in Japanese with English title)

Shigeno, H.: Study on high-temperature hot-springs in the Kinki district, Japan, based on integrated analysis of electronic earth-sciences information (2): Modeling the formation environment at the Yunomine and Arima hot-springs on the bases of plate tectonics. *Chishitsu News*, no. 647, (2008b), 25-38. (in Japanese with English title)

Shigeno, H.: Subduction of the Philippine Sea plat-slab from the Sagami trough area to the Kanto plain, Japan: Simplified modeling and numerical simulation using open electronic earth-sciences information. *Chishitsu News*, no. 648, (2008c), 20-33. (in Japanese with English title)

Shigeno, H.: Relation between spatial-temporal changes of volcanic and geothermal activities in Kyushu, Japan, and subduction of Philippine Sea plat-slab: Simplified modeling and simulation using electronic earth-sciences information. *Chishitsu News*, no. 656, (2009), 10-28. (in Japanese with English title)

Umeda, K., Asamori, K., Oikawa, T., Kakuta, C., Zhao, D. and Kamaya, N.: Geotectonic environment of the geothermal area in the non-volcanic region, southwest Japan. *Chikyu Monthly*, **26**, (2004), 407-413. (in Japanese with English title)

Utsu, T.: *Seismicity Studies: A Comprehensive Review*. University of Tokyo Press, 876p, (1999). (in Japanese with English title)

Uyeda, S.: *Plate Tectonics*. Iwanami Shoten, 268p, (1989). (in Japanese)

Watanabe, Y.: Late Cenozoic evolution of epithermal gold metallogenic provinces in Kyushu, Japan. *Mineralium Deposita*, **40**, (2005), 307-323.

APPENDIX

Some contents of the present article will be improved by the latest results of the author’s studies near future. Refer to the following papers (in press), especially Shigeno (2010) for the Kyushu region.

Shigeno, H.: Pseudo-longitude-latitude coordinate system (PLLCS) for Japanese Islands –An application case study of the Pacific plate subduction beneath the East Japan three-arc system. *Chishitsu News*, no. 664, (2009), 50-61. (in Japanese with English title)

Shigeno, H.: Steepening of slab subduction as a cause of anomalous activities of volcanoes and geothermal systems: Geometry model, and comparisons between the four segmented areas of the Ryukyu and Southwest Japan arcs. *Chishitsu News*, no. 666, (2010), 21-30. (in Japanese with English title)